Structure−Activity Relationships of Acetylcholinesterase Noncovalent Inhibitors Based on a Polyamine Backbone. 3. Effect of Replacing the Inner Polymethylene Chain with Cyclic Moieties

Vincenzo Tumiatti,* Vincenza Andrisano, Rita Banzi, Manuela Bartolini, Anna Minarini, Michela Rosini, and Carlo Melchiorre*

Department of Pharmaceutical Sciences, University of Bologna, Via Belmeloro 6, 40126 Bologna, Italy

Received July 16, 2004

In the present paper we expanded SAR studies of **3**, the ethyl analogue of the AChE inhibitor caproctamine (**2**), by investigating the role of its octamethylene spacer separating the two amide functions through the replacement with dipiperidine and dianiline moieties. Compounds **4** and **8** were the most interesting of the two series of compounds. Compound **4** was the most potent AChE inhibitor with a pIC_{50} value of 8.48 ± 0.02, while displaying also significant muscarinic M_2 antagonistic activity (pK_b value of 6.18 ± 0.20). The availability of a suitable assay allowed us to verify whether **2**, **3**, **4**, and **8** inhibit AChE-induced Aβ aggregation. Although all four derivatives caused a mixed type of AChE inhibition (active site and PAS), only **4** and **8**, which bear an inner constrained spacer, were able to inhibit AChE-induced Aβ aggregation to a greater extent than donepezil. Clearly, the ability of an AChE inhibitor, based on a linear polyamine backbone, to bind both AChE sites may not be a sufficient condition to inhibit also AChE-induced Aβ aggregation. Dipiperidine derivative **4** emerged as a valuable pharmacological tool and a promising lead compound for new ligands to investigate and, hopefully, treat Alzheimer's disease.

Introduction

Alzheimer's disease (AD), the most common form of dementia in adults, is a neurodegenerative disorder characterized by loss of cognitive ability and severe behavioral abnormalities, and it ultimately results in total degradation of intellectual and mental activities.[1] Much effort is devoted to elucidate the relationships among the hallmarks of the disease, that is, amyloid plaques, neurofibrillary tangles, and loss of neurons in the hippocampus and nucleus basalis of Maynart. AD is characterized by a pronounced degradation of the cholinergic system and by alteration in other neurotransmitter systems as glutamatergic and serotoninergic ones.[2]

The actual therapeutic approaches are based on different morphological and biochemical characteristics of AD and focused on the following directions: (i) restoring of the native levels of the cholinergic transmission in CNS; (ii) decreasing the production or aggregation of β-amyloid peptide (Aβ), the major component of the senile plaques, or increasing its removal; (iii) protection of nerve cells from toxic metabolites formed in neurodegenerative processes; (iv) activation of other neurotransmitter systems to compensate indirectly the cholinergic function deficit.

Despite an enormous amount of work, many aspects of both the etiology and the physiological pathway of AD remain still unclear. To date, only acetylcholinesterase (AChE) inhibitors, such as tacrine, donepezil, rivastigmine, and galantamine, and an NMDA receptor antagonist, memantine, are available for AD treatment (Figure 1).[3,4] These drugs have been approved for the symptomatic treatment of AD as they do not even address the etiology of the disease for which are used.[5−7] Some experimental evidence suggests that AChE plays also a noncholinergic function[8,9] in the development of AD. In particular, its consistent presence in senile plaques could represent the cause of Aβ aggregation and deposition.[10,11] It accelerates the assembly of Aβ into insoluble fibrils containing both Aβ and AChE, which are more toxic to cells than Aβ alone.[12] Several studies, carried out in the presence of either competitive or noncompetitive inhibitors of AChE to determine the molecular domain of AChE involved in the interaction

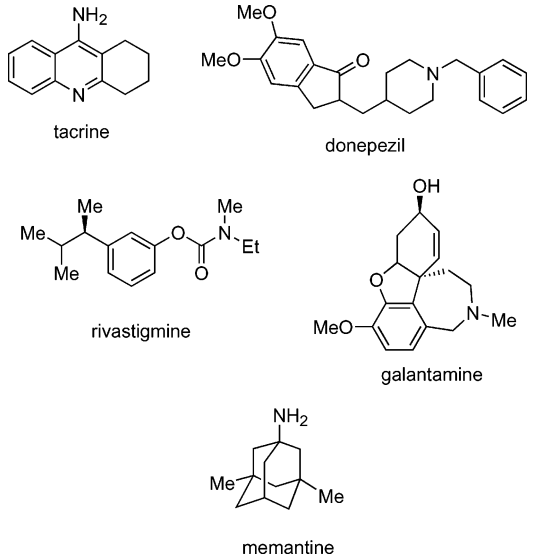

Figure 1. Chemical structure of drugs in current use for the treatment of Alzheimer's disease.

* Corresponding authors. C.M.: tel, +39-051-2099706; fax, +39-051-2099734; e-mail, carlo.melchiorre@unibo.it. V.T.: tel, +39-051-2099709; fax, +39-051-2099734; e-mail, vincenzo.tumiatti@unibo.it.

10.1021/jm0494366 CCC: $27.50
Published on Web 11/16/2004

with Aβ, suggest that the catalytic site of AChE does not participate in the interaction with Aβ. A potential locus of interaction between Aβ and AChE has been identified by crystal structure data on the external surface in proximity of the catalytic gorge of AChE and called the "AChE peripheral site".[13] The specific role of AChE in amyloid formation is confirmed by observations on butyrylcholinesterase (BChE). BChE shares many structural and physicochemical properties with AChE[14] and has been detected in senile plaques and in neurofibrillary tangles, where it is colocalized with the Aβ.[15] However, BChE does not bear a peripheral site and does not enhance the assembly of Aβ into amyloid fibrils.[16,17]

It derives that compounds able to bind simultaneously to both the catalytic and peripheral sites of AChE should implicate advantages over inhibitors that act only on the catalytic site because the inhibition of the peripheral binding site might prevent the aggregation of Aβ induced by AChE. Our group has been involved for a long time in the design and synthesis of ligands having affinity for (i) both AChE active and peripheral binding sites and (ii) muscarinic M_2 receptors[18] by applying the "cholinergic hypothesis".[6] Such derivatives would facilitate ACh release in the synaptic cleft by antagonizing muscarinic M_2 autoreceptors and would potentiate as well the remaining cholinergic transmission in affected brain regions by inhibition of AChE activity.

Application of the universal template approach has allowed us to design polyamines, displaying affinity for AChE and muscarinic M_2 receptors, structurally related to methoctramine (**1**), a well-known selective muscarinic M_2 receptor antagonist.[18,19] It turned out that caproctamine (**2**) antagonized muscarinic M_2 receptors with a pA_2 value of 6.39 and inhibited AChE with a pIC_{50} value of 6.77. Owing to its interesting biological profile, **2** was investigated further by inserting different substituents on the terminal phenyl rings and on the four nitrogen atoms, leading to the *N*-ethyl analogue **3** with a significantly improved inhibitory activity (pIC_{50} = 7.73) toward AChE.

The present article expands on the study of another aspect of structure−activity relationships of **3**, namely the investigation on the role of the octamethylene spacer separating the two amide functions. A previous docking study carried out on the diprotonated form of **2** revealed that **2** is able to interact simultaneously with both active and peripheral sites of AChE and to establish favorable interactions with a number of residues in the gorge thanks to the flexibility of the molecule, which allows it to assume many conformations.[20] To reduce the conformational freedom of the polymethylene chain of polyamines we designed a series of compounds in which the inner octamethylene chain of **3** is incorporated partially or totally into a more constrained moiety as shown in Figure 2.[21] These structural modifications would afford compounds in which the inner diamide moiety is forced to assume a more definite arrangement that would allow the two basic terminal chains to orient themselves in different spatial regions relative to each other. Therefore, the highly flexible polymethylene chain connecting the two amide functions of **3** was replaced by the less flexible dipiperidine or dianiline moieties, affording **4**−**7** or **8**−**10** (Scheme 1), respectively.

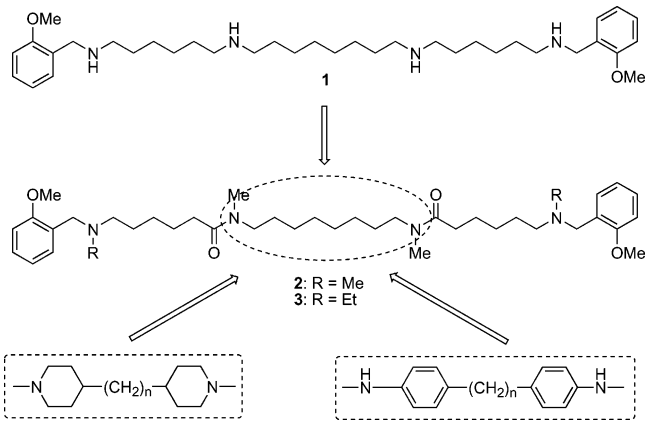

Figure 2. Chemical structure of methoctramine (**1**) and caproctamine (**2**) and of its ethyl analogue **3**. The design strategy for the development of **4**−**16** is also shown.

Since in a previous study we verified that AChE inhibition by polyamines related to **3** was dependent on the extent of protonation of the two terminal amine functions, we included in this study iodomethylated derivatives **11**−**13**, which bear two permanent positive charges to verify further the role of basicity on activity. Finally, to achieve information on the role of the two diamide functions on activity, they were reduced to the corresponding amine functions as in **14**−**16** (Scheme 1). The two inner amine functions of these compounds will be hardly protonated at physiological pH and, consequently, should not alter the overall lipophilicity of the molecule.

Chemistry

All the compounds were synthesized by standard procedures (Scheme 1) and were characterized by IR, ^{1}H NMR, mass spectra, and elemental analysis. Diamine diamides **17**−**20** and **21**−**23** were obtained by reacting *N*-[(benzyloxy)carbonyl]-6-aminocaproic acid with the appropriate dipiperidine or dianiline derivative, respectively. Removal of the *N*-(benzyloxy)carbonyl group by hydrolysis with HBr gave diamine diamides **24**−**30**, which were treated with 2-methoxybenzaldehyde followed by reduction with $NaBH_4$ of the formed Schiff base to the corresponding dibenzyl derivatives **31**−**37**. Diethylation of **31**−**37** to afford **4**−**10** was performed by using diethyl sulfate in toluene at refluxing temperature. The state of the reaction was continuously monitored to avoid possible quaternization of the basic functions. Tetraamines **14**−**16** were prepared by reduction of diamine diamides **8**−**10** with BACH-EI in dry diglyme.

Methiodides **11**−**13** were synthesized by methylation of the corresponding tertiary diamine with an excess of methyl iodide.

Biology

To determine the potential interest of compounds **4**−**16** for the treatment of AD, their inhibitory potency against recombinant human AChE and isolated serum BChE was evaluated by studying the hydrolysis of acetylthiocholine (ATCh) following the method of Ellman et al.[22] The inhibitory potency was expressed as pIC_{50} values, which represent the negative logarithm of the concentration of inhibitor required to decrease

Scheme 1[a]

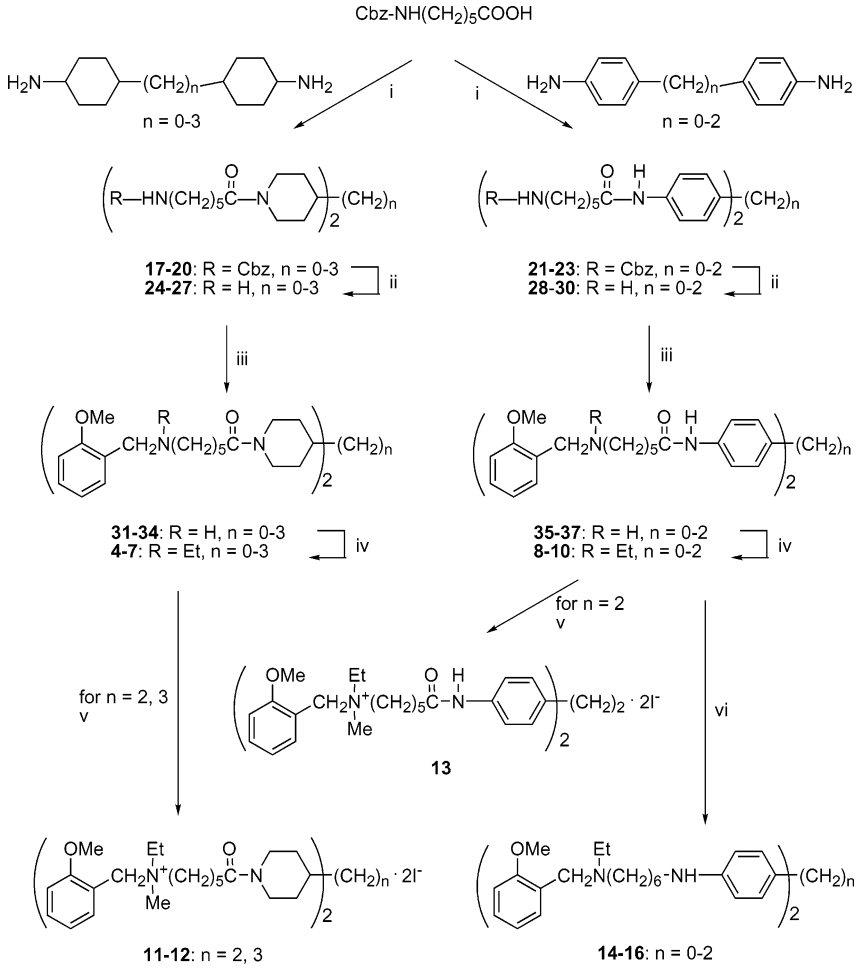

[a] Cbz = $C_6H_5CH_2OCO-$; (i) Et_3N, EtOCOCl, dioxane; (ii) HBr, CH_3COOH; (iii) 2-$MeOC_6H_4CHO$, toluene, $NaBH_4$, EtOH; (iv) $(EtO)_2SO_2$, toluene; (v) CH_3I, acetone; (vi) BACH-EI, diglyme.

enzyme activity by 50%. To allow comparison of the results, **1**−**3**, tacrine, physostigmine, and donepezil were used as the reference compounds. Functional activity of **4** and reference compounds **1**−**3** at muscarinic receptors was determined by the use of the muscarinic M_2 receptor mediated negative inotropism in driven guinea pig left atria (1 Hz).[23] The biological results were expressed as pK_b values according to van Rossum.[24]

The nature of AChE inhibition caused by these compounds was investigated by the comparison of the graphical analysis of steady-state human AChE inhibition data of the most potent compound of this series (**4**) with those of donepezil, a well-known inhibitor of catalytic and peripheral sites of AChE (Figure 3).[25,26]

The ability of compounds **4**, **6**, and **8** to inhibit the proaggregating action of AChE toward Aβ, in comparison with donepezil and reference compounds **2** and **3**, was assessed through a thioflavin T-based fluorometric assay early reported by Inestrosa[27] and recently validated through circular dichroism.[28] The results are reported in Table 1.

Results and Discussion

The inhibitory potency, expressed as pIC_{50} values, of compounds **4**−**16** on human recombinant AChE and BChE from human serum is reported in Table 1 in comparison with the prototype polyamines **1**−**3** and the well-known AChE inhibitors tacrine, physostigmine, and donepezil. Furthermore, compounds **4**, **6**, and **8** were evaluated also for their ability to inhibit the proaggregating action of AChE toward Aβ. Compounds **2**, **3**, and donepezil were used as reference compounds. In addition, the antagonism at muscarinic M_2 receptors was determined for compound **4**.

Recently, we reported that **3** is a potent AChE inhibitor and a muscarinic M_2 receptor antagonist.[21] We demonstrated that the AChE inhibitory potency of polyamines related to **3** is linearly correlated with the basicity of the two basic nitrogen atoms, which is influenced by the nature and the position of substituents on the two aromatic rings. A graphical analysis of steady-state inhibition data indicated that **3** was able to bind at both catalytic and peripheral sites of AChE. Thus, **3** could represent a valuable lead for the design of compounds useful to investigate AD because of (a) their improvement of cholinergic transmission by inhibiting the catalytic site of AChE and (b) their interaction with the AChE peripheral anionic site which might prevent AChE-mediated Aβ aggregation.[21] This reasoning formed the basis for present study. All the synthesized compounds **4**−**16** showed AChE inhibition activity with pIC_{50} values ranging from 4.51 to 8.48. All of the compounds were less potent in inhibiting BChE than AChE activity. The most potent compound against

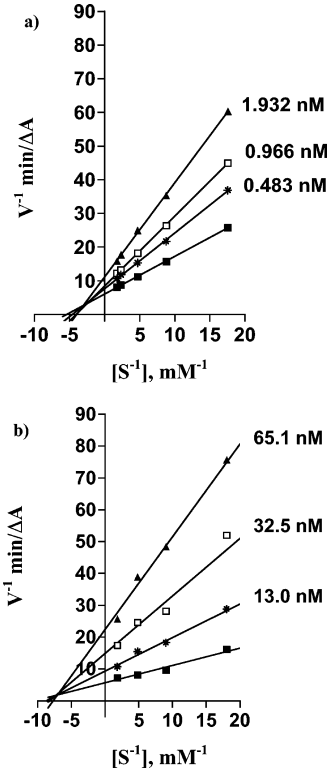

Figure 3. Steady-state inhibition of AChE hydrolysis of acetylthiocholine by **4** (a) and donepezil (b). Reciprocal plot of initial velocity and substrate concentration is reported. Reciprocal plot of initial velocity in the absence of inhibitor gave an estimate of k_{app} for ATCh of 170 ± 15μM (four experiments). Lines were derived from a weighted least-squares analysis of the data points.

BChE was **12** whereas the least active was **16**. Besides AChE inhibition, the observed BChE inhibition may have relevance considering the new emerging role of BChE in AD.[29] An analysis of results reported in Table 1 reveals that AChE inhibition can be markedly affected by the introduction of more constrained spacers, such as dipiperidine and dianiline moieties, in the structure of **3**. The two most potent AChE inhibitors were **4** and **5**, which belong to the dipiperidine series. They displayed also the highest AChE/BChE ratios, which were comparable to each other. Compounds **6** and **7**, which bear a longer spacer in their structure, were only twice less potent than **4** at AChE, whereas they resulted slightly more potent in inhibiting BChE activity. The quaternization of **4** and **5**, leading to **11** and **12,** did not improve AChE and BChE inhibitory activity, suggesting that the 2-methoxy functions on the two aromatic rings are endowed with optimal electronic properties, in agreement with previous results obtained with polyamines related to **3**.

Replacing the 1,8-diaminooctane spacer of **3** with a dianiline moiety, leading to **8**−**10**, caused a decrease in inhibitory activity on AChE as well as in the selectivity AChE/BChE ratio. The most potent inhibitor of this series was **8**, which is endowed of the shortest distance between the two amide functions, confirming the trend observed for the dipiperidine series. Again, the quaternization of the two basic nitrogen atoms of **10**, leading to **13**, did not affect the inhibitory activity on AChE as observed for the dipiperidine series.

The reduction of the two amide functions of **8**−**10**, leading to compounds **14**−**16**, caused a marked loss in activity, confirming a previous finding that polymethylene tetraamines are less active on AChE than the corresponding diamine diamides (for example, compare the inhibitory potency of **1** vs **2**). The finding that **4** and **8**, which are endowed of the shortest distance (n = 0, Table 1) between the two amide nitrogen atoms in the dipiperidine and dianiline series, respectively, showed the highest potency within the two series may indicate that the octamethylene spacer of **3** interacts with AChE in a not extended conformation.

The graphical analysis of steady-state inhibition data for **4** in comparison to donepezil is shown in Figure 3, whereas the estimates of competitive inhibition constants K_i of derivatives **2**, **3**, **4**, and donepezil are reported in Table 2. It was found that **4**, like **2**, **3**, and donepezil, caused a mixed type inhibition, that is, inhibition of both the catalytic site and a second distal site of the enzyme, according to the reported results indicating that donepezil is a double site inhibitor.[25] In addition, an analysis of K_i values shown in Table 2 reveals that **4** is the most potent among the investigated diamine diamides.

Furthermore, the availability of a suitable test for the determination of the Aβ aggregation induced by AChE allowed us to verify if an inhibitor of peripheral and active sites of AChE is able to decrease or block the Aβ aggregation induced by AChE. To this end, we selected compounds **4**/**8** and **6** because they have a shorter or a longer spacer, respectively, in comparison to prototype **2**, **3**, and donepezil. It turned out that reference compounds **2** and **3** were not able to inhibit the Aβ aggregation induced by AChE, although the steady-state diagrams of AChE inhibition confirmed the binding of the two ligands to both active and peripheral AChE sites, whereas **4** showed a 41% inhibition that was significantly higher than the percent inhibition (22%) observed for donepezil. Interestingly, **4** was more potent than **6** (15%) in inhibiting AChE-induced Aβ aggregation, which may suggest that optimal inhibition is achieved when the two rings of the inner spacer are linked to each other, giving raise to a more rigid structure. This view was in agreement with the inhibition value of 35% observed for **8**, which bears a dianiline spacer. The finding that **2** and **3**, although binding to both AChE sites, did not affect Aβ aggregation may indicate that the ability to bind to active and peripheral sites of AChE is not a sufficient condition to inhibit the Aβ aggregation induced by AChE. It appears that to inhibit Aβ aggregation a **2**-related polyamine must incorporate in its structure a constrained spacer between the two inner nitrogen atoms, rather than a flexible polymethylene chain.

Interestingly diamine diamide **4** besides its AChE and Aβ-aggregation inhibition properties was also a muscarinic M_2 receptor antagonist in the guinea pig left atrium (pK_b = 6.18 ± 0.20). This additional property may help in increasing ACh release in the synapse as a result of muscarinic M_2 autoreceptors blockade.

Conclusions

The present investigation has demonstrated that the replacement of the inner linear polymethylene chain of

Table 1. Inhibition of AChE and BChE Activities and AChE-Induced Aβ Aggregation by Polyamines

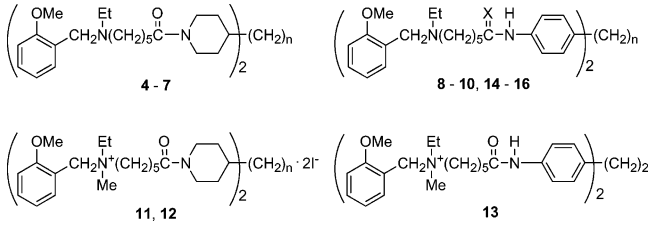

no.[a]	X	n	pIC_{50}[b] AChE	pIC_{50}[b] BChE	AChE/BChE[c]	$pK_b(M_2)$[d]	% inhibition of Aβ aggregation[e]
1[f]			5.27 ± 0.03	6.01 ± 0.02	0.2	7.92 ± 0.08[g]	nd[h]
2[f]			6.77 ± 0.01	4.93 ± 0.04	68	6.39 ± 0.23[g]	<5[i]
3[f]			7.73 ± 0.02	5.65 ± 0.03	121	5.65 ± 0.6[g]	<5[i]
4		0	8.48 ± 0.02	5.07 ± 0.03	2570	6.18 ± 0.20	41 ± 2
5		1	8.48 ± 0.01	5.19 ± 0.03	1949	nd	nd
6		2	8.13 ± 0.02	5.44 ± 0.02	490	nd	15 ± 3
7		3	8.18 ± 0.03	5.47 ± 0.02	513	nd	nd
8	O	0	7.44 ± 0.03	5.73 ± 0.02	51	nd	35 ± 5
9	O	1	7.20 ± 0.03	5.74 ± 0.03	29	nd	nd
10	O	2	6.77 ± 0.02	5.77 ± 0.01	10	nd	nd
11		2	8.24 ± 0.02	5.73 ± 0.01	323	nd	nd
12		3	8.24 ± 0.02	6.18 ± 0.02	115	nd	nd
13			6.92 ± 0.03	5.96 ± 0.06	9	nd	nd
14	H_2	0	5.58 ± 0.01	4.81 ± 0.02	6	nd	nd
15	H_2	1	5.97 ± 0.04	5.79 ± 0.06	2	nd	nd
16	H_2	2	4.51 ± 0.05	4.02 ± 0.04	3	nd	nd
tacrine			6.37 ± 0.02	7.34 ± 0.02	0.1	nd	nd
physostigmine			7.87 ± 0.18	7.58 ± 0.15	2	nd	nd
donepezil			7.64 ± 0.09	5.12 ± 0.01	331	nd	22 ± 3

[a] **1**, tetrahydrochloride; **2**−**10**, dioxalate; **11**−**13**, methiodides. [b] Human recombinant AChE and BChE from human serum were used. pIC_{50} values represent the negative logarithm of the concentration of inhibitor required to decrease enzyme activity by 50% and are the mean of two independent measurements, each performed in triplicate. [c] The AChE/BChE selectivity ratio is the antilog of the difference between pIC_{50} values at AChE and BChE, respectively. [d] pK_b values (±SE, $n = 4$) were calculated according to Van Rossum[24] at 10 μM concentration at muscarinic M_2 receptors in guinea pig left atrium. [e] Inhibition of AChE-induced Aβ aggregation produced by the tested compound at 100 μM concentration. [f] See Figure 2 for structure. [g] Data from ref 21. [h] Not determined. [i] Not significant.

Table 2. Inhibition Constants of AChE Obtained with **4** in Comparison with **2**, **3**, and Donepezil[a]

compd	AChE K_i (nM)
2	104 ± 0.6[b]
3	12.2 ± 16[c]
4	5.67 ± 0.15
donepezil	20.5 ± 3.3[d]

[a] Inhibition constants, expressed as pK_i values, were calculated from kinetic data in Figure 3. [b] Data from ref 20. [c] Data from ref 21. [d] Data from ref 26.

2 and **3** with a bicyclic moiety led to an increase of AChE inhibitory activity. The most active compounds of this new series of polyamines were dipiperidines **4** and **5**, and the dianiline **8**, which are endowed of the shortest distance between the two amide functions. These data may indicate that **2** and **3** interact in a not extended conformation with AChE.

The analysis of steady-state diagrams of **2**, **3**, **4**, and **8** showed that all derivatives caused inhibition of AChE catalytic and peripheral sites (dual sites), but only **4** and **8**, which incorporate in their polyamine backbone an inner constrained spacer, were able to inhibit AChE-induced Aβ aggregation to a greater extent than the reference compound donepezil. Thus, it is our hypothesis that inhibition of AChE peripheral site is not a sufficient condition to inhibit AChE-induced Aβ aggregation, which may necessitate particular structural requirements to prevent the interaction of AChE with Aβ. Derivative **4** was also a muscarinic M_2 antagonist, a property that can enhance the release of AChE in the synaptic cleft. Owing to its biological profile, **4** may represent a new promising lead in the field of AD.

Experimental Section

Chemistry. Melting points were taken in glass capillary tubes on a Buechi SMP-20 apparatus and are uncorrected. Electron impact (EI) mass and direct infusion ESI-MS spectra were recorded on VG 7070E, and Waters ZQ 4000 apparatus, respectively. ^{1}H NMR spectra were recorded on a Varian VXR 300 instrument. Chemical shifts are reported in parts per million (ppm) relative to tetramethylsilane (TMS), and spin multiplicities are given as s (singlet), br s (broad singlet), d (doublet), q (quartet), t (triplet), or m (multiplet). The elemental compositions of the compounds agreed to within ±0.4% of the calculated value. When the elemental analysis is not included, crude compounds were used in the next step without further purification. Chromatographic separations were performed on silica gel columns by flash (Kieselgel 40, 0.040−0.063 mm; Merck) or gravity column (Kieselgel 60, 0.063−0.200 mm; Merck) chromatography. Reactions were followed by thin-layer chromatography (TLC) on Merck (0.25 mm) glass-packed precoated silica gel plates (60 F254) that were visualized in an iodine chamber. The term "dried" refers to the use of anhydrous sodium sulfate. Compounds were named following IUPAC rules as applied by Beilstein-Institut AutoNom (version 2.1), a PC integrated software package for systematic names in organic chemistry.

General Procedures for the Synthesis of {6-[1′-(6-Benzyloxycarbonylamino-hexanoyl)-[4,4′]bipiperidinyl-1-yl]-6-oxo-hexyl}-carbamic Acid Benzyl Ester (17), (6-{4-[1-(6-Benzyloxycarbonylamino-hexanoyl)-piperidin-4-ylmethyl]-piperidin-1-yl}-6-oxo-hexyl)-carbamic Acid Benzyl Ester (18), [6-(4-{2-[1-(6-Benzyloxycarbonylamino-hexanoyl)-piperidin-4-yl]-ethyl}-piperidin-1-yl)-6-oxo-hexyl] Carbamic Acid Benzyl Ester (19), [6-(4-{3-[1-(6-

Benzyloxycarbonylamino-hexanoyl)-piperidin-4-yl]-propyl}-piperidin-1-yl)-6-oxo-hexyl]-carbamic Acid Benzyl Ester (20), {5-[4′-(6-Benzyloxycarbonylamino-hexanoylamino)-biphenyl-4-ylcarbamoyl]-pentyl}-carbamic Acid Benzyl Ester (21), (5-{4-[4-(6-Benzyloxycarbonylamino-hexanoylamino)-benzyl]-phenylcarbamoyl}-pentyl)-carbamic Acid Benzyl Ester (22), and [5-(4-{2-[4-(6-Benzyloxycarbonylamino-hexanoylamino)-phenyl]-ethyl}-phenylcarbamoyl)-pentyl]-carbamic Acid Benzyl Ester (23). Ethyl chloroformate (0.95 mL, 10 mmol) in dry dioxane (20 mL) was added dropwise to a stirred and cooled (5 °C) solution of *N*-[(benzyloxy)carbonyl]-6-aminocaproic acid (2.65 g, 10 mmol) and triethylamine (1.4 mL, 10 mmol) in dioxane (30 mL), followed after standing for 30 min by the addition of the suitable dipiperidine or dianiline (5 mmol) in dioxane (20 mL). After the mixture was stirred at room temperature for 72 h, the solvent was evaporated, affording a residue that was suspended in water (100 mL). The aqueous mixture was extracted with $CHCl_3$ (4 × 20 mL) or the solid residue filtered off for compounds **21**−**23**. The organic phase or the solid residue for **21**−**23** was washed with 2 N NaOH, 2 N HCl, and brine. Removal of the dried solvent gave the desired crude products **17**−**23**.

17: white powder; 82% yield from [4,4′]dipiperidine as starting diamine and purified by gravity chromatography eluting with CH_2Cl_2/EtOAc/EtOH (6.5:3:0.5); mp 95−98 °C; ^{1}H NMR ($CDCl_3$) δ 0.91−1.75 (m, 22H), 2.12−2.42 (m, 6H), 2.82 (t, 2H), 3.08 (d, 4H), 3.75 (d, 2H), 4.48 (d, 2H), 5.01 (s, 4H), 5.45 (br s, 2H exchangeable with D_2O), 7.05−7.23 (m, 10H).

18: white powder; 48% yield from 4-(piperidin-4-ylmethyl)-piperidine as starting diamine and purified by flash chromatography eluting with $CHCl_3$/EtOAc/CH_3OH (7.5:2:0.5); mp 99−101 °C; ^{1}H NMR (CD_3OD) δ 0.98−1.91 (m, 24H), 2.38 (t, 4H), 2.61 (t, 2H), 2.98−3.19 (m, 6H), 3.85−4.02 (m, 2H), 4.42−4.58 (m, 2H), 5.08 (s, 4H), 7.28−7.40 (m, 10H), 7.95 (s, 2H exchangeable with D_2O).

19: white powder; 59% yield from 4-(2-piperidin-4-ylethyl)-piperidine as starting diamine and purified by flash chromatography eluting with CH_2Cl_2/EtOAc/CH_3OH (6:3.7:0.3); mp 118−120 °C; ^{1}H NMR ($CDCl_3$) δ 1.02−1.78 (m, 26H), 2.33 (t, 4H), 2.51 (t, 2H), 2.98 (t, 2H), 3.24 (q, 4H), 3.81 (d, 2H), 4.62 (d, 2H), 4.85 (br s, 2H exchangeable with D_2O), 5.11 (s, 4H), 7.28−7.42 (m, 10H).

20: white powder; 23% yield from 4-(3-piperidin-4-ylpropyl)-piperidine as starting diamine and purified by flash chromatography eluting with CH_2Cl_2/EtOAc/CH_3OH (8.5:0.5:1); mp 90−91 °C; ^{1}H NMR ($CDCl_3$) δ 0.95−1.72 (m, 28H), 2.29 (t, 4H), 2.48 (t, 2H), 2.94 (t, 2H), 3.12−3.21 (m, 4H), 3.79 (d, 2H), 4.58 (d, 2H), 4.82 (br s, 2H exchangeable with D_2O), 5.10 (s, 4H), 7.25−7.40 (m, 10H).

21: white powder; nearly quantitative yield from biphenyl-4,4′-diamine as starting diamine; mp 279−281 °C dec; ^{1}H NMR (DMSO-d_6) δ 1.15−1.61 (m, 12H), 2.28 (t, 4H), 2.96 (t, 4H), 4.96 (s, 4H), 7.20−7.35 (m, 10H + 2H exchangeable with D_2O), 7.52−7.64 (m, 8H), 10.01 (s, 2H exchangeable with D_2O).

22: white powder; 83% yield from 4-(4-aminobenzyl)aniline as starting diamine; mp 178−179 °C; ^{1}H NMR (DMSO-d_6) δ 1.17−1.60 (m, 12H), 2.18 (t, 4H), 2.94 (q, 4H), 3.76 (s, 2H), 4.95 (s, 4H), 7.05 (d, 4H), 7.17−7.37 (m, 10H + 2H exchangeable with D_2O), 7.43 (d, 4H), 9.94 (s, 2H exchangeable with D_2O).

23: white powder; nearly quantitative yield using 4-(4-aminophenethyl)aniline as starting diamine; mp 184−185 °C; ^{1}H NMR (DMSO-d_6) δ 1.20−1.61 (m, 12H), 2.26 (t, 4H), 2.77 (s, 4H), 2.98 (q, 4H), 5.00 (s, 4H), 6.62 (d, 1H exchangeable with D_2O), 6.85 (d, 1H exchangeable with D_2O), 7.09 (d, 4H), 7.30−7.40 (m, 10H), 7.47 (d, 4H), 9.78 (s, 2H exchangeable with D_2O).

General Procedures for the Synthesis of 6-Amino-1-[1′-(6-amino-hexanoyl)-[4,4′]bipiperidinyl-1-yl]-hexan-1-one (24), 6-Amino-1-{4-[1-(6-amino-hexanoyl)-piperidin-4-ylmethyl]-piperidin-1-yl}-hexan-1-one (25), 6-Amino-1-(4-{2-[1-(6-amino-hexanoyl)-piperidin-4-yl]-ethyl}-piperidin-1-yl)-hexan-1-one (26), 6-Amino-1-(4-{3-[1-(6-amino-hexanoyl)-piperidin-4-yl]-propyl}-piperidin-1-yl)-hexan-1-one (27), 6-Amino-hexanoic Acid [4′-(6-amino-hexanoylamino)-biphenyl-4-yl]-amide (28), 6-Amino-hexanoic Acid {4-[4-(6-amino-hexanoylamino)-benzyl]-phenyl}-amide (29), and 6-Amino-hexanoic Acid (4-{2-[4-(6-amino-hexanoylamino)-phenyl]-ethyl}-phenyl)-amide (30). A solution of 30% HBr in acetic acid (25 mL) was added to a solution of **17**−**23** (3.1 mmol) in acetic acid, and the resulting mixture was stirred for 4 h at room temperature. Ether (100 mL) was then added, yielding an oil, which was washed with ether (3 × 20 mL) and dissolved in water (50 mL). The solution was made basic with KOH pellets and extracted with $CHCl_3$ (3 × 30 mL). Removal of the dried solvent gave compounds **24**−**30** in quantitative yields.

24: foam solid; ^{1}H NMR ($CDCl_3$, free base) δ 0.98−1.83 (m, 22H + 4H exchangeable with D_2O), 2.23 (t, 4H), 2.38 (t, 2H), 2.64 (t, 4H), 2.88 (t, 2H), 3.81 (d, 2H), 4.58 (d, 2H).

25: foam solid; ^{1}H NMR ($CDCl_3$, free base) δ 0.98−1.78 (m, 24H + 4H exchangeable with D_2O), 2.31 (t, 4H), 2.52 (t, 2H), 2.68 (t, 4H), 2.98 (t, 2H), 3.82 (d, 2H), 4.58 (d, 2H).

26: foam solid; ^{1}H NMR ($CDCl_3$, free base) δ 0.73−1.42 (m, 26H), 1.91−2.08 (m, 4H), 2.18 (br s, 4H exchangeable with D_2O), 2.38 (t, 4H), 2.68 (t, 4H), 3.51 (d, 2H), 4.23 (d, 2H).

27: foam solid; ^{1}H NMR ($CDCl_3$, free base) δ 0.95−1.72 (m, 28H), 2.28 (t, 4H), 2.42−2.54 (m, 2H + 4H exchangeable with D_2O), 2.68 (t, 4H), 2.93 (t, 2H), 3.80 (d, 2H), 4.55 (d, 2H).

28: mp 280 °C dec; ^{1}H NMR (DMSO-d_6, free base) δ 1.22−1.75 (m, 12H), 2.25 (t, 4H), 2.35−2.48 (m, 4H), 3.10 (br s, 4H exchangeable with D_2O), 7.51−7.89 (m, 8H), 9.93 (s, 2H exchangeable with D_2O).

29: mp 130−132 °C; ^{1}H NMR (DMSO-d_6, free base) δ 1.18−1.60 (m, 12H), 2.26 (t, 4H), 2.42−2,56 (m, 4H), 3.21 (br s, 4H exchangeable with D_2O), 3.80 (s, 2H), 7.01−7.56 (m, 8H), 9.78 (s, 2H exchangeable with D_2O).

30: mp 174−175 °C; ^{1}H NMR (DMSO-d_6, free base) δ 1.20−1.61 (m, 12H), 2.27 (t, 4H), 2.44−2.57 (m, 4H), 2.77 (s, 4H), 3.25 (br s, 4H exchangeable with D_2O), 7.09 (d, 4H), 7.48 (d, 4H), 9.78 (s, 2H exchangeable with D_2O).

General Procedures for the Synthesis of 6-(2-Methoxy-benzylamino)-1-{1′-[6-(2-methoxy-benzylamino)-hexanoyl]-[4,4′]bipiperidinyl-1-yl}-hexan-1-one (31), 6-(2-Methoxy-benzylamino)-1-(4-{1-[6-(2-methoxy-benzylamino)-hexanoyl]-piperidin-4-ylmethyl}-piperidin-1-yl)-hexan-1-one (32), 6-(2-Methoxy-benzylamino)-1-[4-(2-{1-[6-(2-methoxy-benzylamino)-hexanoyl]-piperidin-4-yl}-ethyl)-piperidin-1-yl]-hexan-1-one (33), 6-(2-Methoxy-benzylamino)-1-[4-(3-{1-[6-(2-methoxy-benzylamino)-hexanoyl]-piperidin-4-yl}-propyl)-piperidin-1-yl]-hexan-1-one (34), 6-(2-Methoxy-benzylamino)-hexanoic Acid {4′-[6-(2-Methoxy-benzylamino)-hexanoylamino]-biphenyl-4-yl}-amide (35), 6-(2-Methoxy-benzylamino)-hexanoic Acid (4-{4-[6-(2-Methoxy-Benzylamino)-hexanoylamino]-benzyl}-phenyl)-amide (36), and 6-(2-Methoxy-benzylamino)-hexanoic Acid [4-(2-{4-[6-(2-Methoxy-benzylamino)-hexanoylamino]-phenyl}-ethyl)-phenyl]-amide (37). A mixture of **24**−**30** and 2-methoxybenzaldehyde (in a 1:2.2 molar ratio) in toluene (50 mL) was stirred at the refluxing temperature in a Dean−Stark apparatus for 6 h. Following solvent removal, the residue was taken up in EtOH (30 mL), $NaBH_4$ was added, and the stirring was continued at room temperature for 6 h. The mixture was then made acidic with 3 N HCl, filtered, and evaporated. The residue was dissolved in water, and the resulting solution was washed with ether, made basic with 2 N NaOH, and extracted with $CHCl_3$. Removal of the dried solvent gave the desired crude products **31**−**37**, which, when necessary, were purified by flash chromatography.

31: pale yellow oil; 78% yield; ^{1}H NMR ($CDCl_3$) δ 0.98−1.80 (m, 22H), 2.18 (br s, 2H exchangeable with D_2O), 2.28−2.38 (m, 4H), 2.45 (t, 2H), 2.64 (t, 4H), 2.88 (t, 2H), 3.78 (s, 4H), 3.82−3.91 (m, 8H), 4.64 (d, 2H), 6.82−6.95 (m, 4H), 7.21−7.31 (m, 4H).

32: pale yellow oil; 85% yield; ^{1}H NMR ($CDCl_3$) δ 0.98−1.83 (m, 24H), 2.22−2.38 (m, 4H + 2H exchangeable with D_2O),

2.43−2.71 (m, 6H), 2.96 (t, 2H), 3.75−3.89 (m, 12H), 4.62 (d, 2H), 6.81−7.31 (m, 8H); EI MS *m/z* 648 (M^+).

33: pale yellow oil; 85% yield; eluting solvent CH_2Cl_2/EtOAc/CH_3OH/aqueous 30% ammonia (6:3:1:0.2); ^1H NMR ($CDCl_3$) δ 0.95−1.72 (m, 26H), 1.98 (br s, 2H exchangeable with D_2O), 2.27 (t, 4H), 2.48 (t, 2H), 2.56 (t, 4H), 2.94 (t, 2H), 3.74−3.82 (m, 12H), 4.56 (d, 2H), 6.80−6.90 (m, 4H), 7.16−7.24 (m, 4H); EI MS *m/z* 662 (M^+).

34: pale yellow oil; 88% yield; eluting solvent CH_2Cl_2/EtOAc/CH_3OH/aqueous 30% ammonia (5:4:1:0.1); ^1H NMR ($CDCl_3$) δ 0.80−1.65 (m, 28H + 2H exchangeable with D_2O), 2.20 (t, 4H), 2.25−2.53 (m, 6H), 2.81 (t, 2H), 3.68−3.71 (m, 12H), 4.49 (d, 2H), 6.71−6.82 (m, 4H), 7.09−7.17 (m, 4H).

35: colorless oil; 56% yield; purified by gravity column eluting with CH_3OH/toluene/aqueous 30% ammonia (7:3:0.1); ^1H NMR ($CDCl_3$) δ 1.35−1.81 (m, 12H + 2H exchangeable with D_2O), 2.39 (t, 4H), 2.64 (t, 4H), 3.81 (s, 4H), 3.84 (s, 6H), 6.84−6.98 (m, 4H), 7.18−7.38 (m, 4H), 7.48−7.68 (m, 8H + 2H exchangeable with D_2O).

36: colorless oil; 43% yield; purified by gravity column eluting with CH_3OH/toluene/aqueous 30% ammonia (6:4:0.1); ^1H NMR ($CDCl_3$) δ 1.31−1.78 (m, 12H), 2.01 (br s, 2H exchangeable with D_2O), 2.29 (t, 4H), 2.61 (t, 4H), 3.79 (s, 4H), 3.82 (s, 6H), 3.87 (s, 2H), 6.82−6.93 (m, 4H), 7.03 (d, 4H), 7.18−7.25 (m, 4H), 7.38 (d, 4H), 8.10 (s, 2H exchangeable with D_2O).

37: colorless oil; 27% yield; eluting solvent $CHCl_3$/CH_3OH/petroleum ether/toluene/aqueous 30% ammonia (5:2:2:1:0.15); ^1H NMR ($CDCl_3$) δ 1.18−1.76 (m, 12H), 1.95 (br s, 2H exchangeable with D_2O), 2.26 (t, 4H), 2.57 (t, 4H), 2.81 (s, 4H), 3.73 (s, 4H), 3.82 (s, 6H), 6.82−6.98 (m, 4H), 7.08 (d, 4H), 7.14−7.25 (m, 4H), 7.34 (d, 4H), 7.94 (br s, 2H exchangeable with D_2O).

General Procedure for the Synthesis of 6-[Ethyl-(2-methoxy-benzyl)-amino]-1-(1′-{6-[ethyl-(2-methoxy-benzyl)-amino]-hexanoyl}-[4,4′]bipiperidinyl-1-yl)-hexan-1-one (4), 6-[Ethyl-(2-methoxy-benzyl)-amino]-1-[4-(1-{6-[ethyl-(2-methoxy-benzyl)-amino]-hexanoyl}-piperidin-4-ylmethyl)-piperidin-1-yl]-hexan-1-one (5), 6-[Ethyl-(2-methoxy-benzyl)-amino]-1-{4-[2-(1-{6-[ethyl-(2-methoxy-benzyl)-amino]-hexanoyl}-piperidin-4-yl)-ethyl]-piperidin-1-yl}-hexan-1-one (6), 6-[Ethyl-(2-methoxy-benzyl)-amino]-1-{4-[3-(1-{6-[ethyl-(2-methoxy-benzyl)-amino]-hexanoyl}-piperidin-4-yl)-propyl]-piperidin-1-yl}-hexan-1-one (7), 6-[Ethyl-(2-methoxy-benzyl)-amino]-hexanoic Acid (4′-{6-[Ethyl-(2-methoxy-benzyl)-amino]-hexanoylamino}-biphenyl-4-yl)-amide (8), 6-[Ethyl-(2-methoxy-benzyl)-amino]-hexanoic Acid [4-(4-{6-[Ethyl-(2-methoxy-benzyl)-amino]-hexanoylamino}-benzyl)-phenyl]-amide (9), and 6-[Ethyl-(2-methoxy-benzyl)-amino]-hexanoic Acid {4-[2-(4-{6-[Ethyl-(2-methoxy-benzyl)-amino]-hexanoylamino}-phenyl)-ethyl]-phenyl}-amide (10). A mixture of **31**−**37** and diethyl sulfate (1:2.5 ratio) was refluxed for 48 h in toluene. Following removal of the solvent, the residue was taken up in water, made basic with KOH pellets, and immediately extracted with $CHCl_3$ (3 × 20 mL) or directly purified by column chromatography to avoid the quaternization of the amine functions. Removal of the dried solvent gave a residue, which was purified by flash chromatography. All the purified compounds were converted in dioxalate salt (foam solid).

4: 35% yield; eluting solvent CH_2Cl_2/EtOAc/CH_3OH/aqueous 30% ammonia (6:3:1:0.05); ^1H NMR (free base, $CDCl_3$) δ 1.15 (t, 6H), 1.12−1.82 (m, 22H), 2.31 (t, 4H), 2.42−2.71 (m, 10H), 2.93 (t, 2H), 3.78 (s, 4H), 3.81−3.96 (m, 8H), 4.65 (d, 2H), 6.83−7.02 (m, 4H), 7.22−7.35 (m, 2H), 7.45 (d, 2H); EI MS *m/z* 691 (M^+). Anal. ($C_{46}H_{70}N_4O_{12}$) C, H, N.

5: 17% yield; eluting solvent CH_2Cl_2/EtOAc/CH_3OH/aqueous 30% ammonia (5:4:1:0.10); ^1H NMR (free base, $CDCl_3$) δ 1.08 (t, 6H), 1.18−1.73 (m, 24H), 2.25 (t, 4H), 2.32−2.73 (m, 10H), 2.93 (t, 2H), 3.73 (s, 4H), 3.78−3.84 (m, 8H), 4.58 (d, 2H), 6.78−6.94 (m, 4H), 7.22 (t, 2H), 7.43 (d, 2H); EI MS *m/z* 705 (M + 1). Anal. ($C_{47}H_{72}N_4O_{12}$) C, H, N.

6: 21% yield; eluting solvent CH_2Cl_2/CH_3OH (7:3); ^1H NMR (free base $CDCl_3$) δ 1.06 (t, 6H), 1.12−1.78 (m, 26H), 2.31 (t, 4H), 2.45−2.59 (m, 10H), 2.97 (t, 2H), 3.58−3.89 (m, 12H), 4.60 (d, 2H), 6.81−7.00 (m, 4H), 7.22 (t, 2H), 7.42 (d, 2H); EI MS *m/z* 718 (M^+). Anal. ($C_{48}H_{74}N_4O_{12}$) C, H, N.

7: 10% yield; eluting solvent CH_2Cl_2/CH_3OH (7:3); ^1H NMR (free base, $CDCl_3$) δ 1.07 (t, 6H), 1.12−1.65 (m, 28H), 2.28 (t, 4H), 2.43−2.58 (m, 10H), 2.92 (t, 2H), 3.60 (s, 4H), 3.77−3.83 (m, 8H), 4.59 (d, 2H), 6.80−6.95 (m, 4H), 7.21 (t, 2H), 7.40 (d, 2H); EI MS *m/z* 732 (M^+). Anal. ($C_{49}H_{76}N_4O_{12}$) C, H, N.

8: 44% yield; eluting solvent CH_2Cl_2/EtOAc/CH_3OH/aqueous 30% ammonia (5:4:1:0.05); ^1H NMR (free base, $CDCl_3$) δ 1.07 (t, 6H), 1.25−1.80 (m, 12H), 2.31−2.63 (m, 12H), 3.62 (s, 4H), 3.82 (s, 6H), 6.83−6.98 (m, 4H), 7.18−7.59 (m, 12H), 7.88 (s, 2H exchangeable with D_2O); EI MS *m/z* 707 (M + 1). Anal. ($C_{48}H_{62}N_4O_{12}$) C, H, N.

9: 16% yield; eluting solvent CH_2Cl_2/EtAc/MeOH/aqueous 30% ammonia (5:4:1:0.06); ^1H NMR (free base, $CDCl_3$) δ 1.04 (t, 6H), 1.20−1.75 (m, 12H), 2.29 (t, 4H), 2.44−2.58 (m, 8H), 3.59 (s, 4H), 3.79 (s, 6H), 3.87 (s, 2H), 6.81−6.95 (m, 4H), 7.08 (d, 4H), 7.18−7.22 (m, 4H), 7.36−7.41 (m, 4H + 2H exchangeable with D_2O); EI MS *m/z* 721 (M + 1). Anal. ($C_{49}H_{64}N_4O_{12}$) C, H, N.

10: 49% yield; eluting solvent CH_2Cl_2/EtAc/MeOH/aqueous 30% ammonia (5:4:1:0.15); ^1H NMR (free base, $CDCl_3$) δ 1.03 (t, 6H), 1.25−1.79 (m, 12H), 2.30 (t, 4H), 2.44−2.56 (m, 8H), 2.83 (s, 4H), 3.58 (s, 4H), 3.80 (s, 6H), 6.84−6.99 (m, 4H), 7.08 (d, 4H), 7.10−7.31 (m, 4H), 7.38−7.46 (m, 4H + 2H exchangeable with D_2O); EI MS *m/z* 735 (M + 1). Anal. ($C_{50}H_{66}N_4O_{12}$) C, H, N.

General Procedures for the Synthesis of *N*4,*N*4′-Bis-{6-[ethyl-(2-methoxy-benzyl)-amino]-hexyl}-biphenyl-4,4′-diamine (14), *N*-Ethyl-*N*′-[4-(4-{6-[ethyl-(2-methoxy-benzyl)-amino]-hexylamino}-benzyl)-phenyl]-*N*-(2-methoxy-benzyl)-hexane-1,6-diamine (15), and *N*-Ethyl-*N*′-{4-[2-(4-{6-[ethyl-(2-methoxy-benzyl)-amino]-hexylamino}-phenyl)-ethyl]-phenyl}-*N*-(2-methoxy-benzyl)-hexane-1,6-diamine (16). A solution of 2 M BACH-EI in tetrahydrofuran (0.9 mL) was added dropwise at room temperature to a solution of **8**−**10** (0.4 mmol) in dry diglyme (10 mL) under a stream of dry nitrogen. When the addition was completed, the reaction mixture was heated at 200 °C for 2 h. After cooling at room temperature, excess borane was destroyed by cautious dropwise addition of 2 N HCl (3 mL) and water (2 mL). The resulting mixture was then heated at 200 °C for 1 h. After cooling at 0 °C, the mixture was made basic with KOH powder and extracted with $CHCl_3$ (3 × 50 mL). Removal of the dried solvent gave a residue, which was purified by gravity column chromatography. All the purified compounds were converted in dioxalate salts (foam solid).

14: colorless oil; 47% yield; eluting solvent CH_2Cl_2/EtOAc/petroleum ether/CH_3OH/aqueous 30% ammonia (4.5:2:3:0.5:0.09); ^1H NMR ($CDCl_3$) δ 1.08 (t, 6H), 1.21−1.78 (m, 16H + 2H exchangeable with D_2O), 2.38−2.41 (m, 8H), 3.11 (t, 4H), 3.62 (s, 4H), 3.82 (s, 6H), 6.61 (d, 4H), 6.72−7.01 (m, 4H), 7.08−7.25 (m, 8H); EI MS *m/z* 679 (M + 1). Anal. ($C_{48}H_{66}N_4O_{10}$) C, H, N.

15: colorless oil; 38% yield; eluting solvent $CHCl_3$/EtOAc/petroleum ether/CH_3OH/aqueous 30% ammonia (4:3:2.5:0.5:0.05); ^1H NMR ($CDCl_3$) δ 1.12 (t, 6H), 1.22−1.71 (m, 16H + 2H exchangeable with D_2O), 2.41−2.62 (m, 8H), 3.11 (t, 4H), 3.61 (s, 4H), 3.78 (s, 2H), 3.83 (s, 6H), 6.58 (d, 4H), 6.82−7.12 (m, 8H), 7.17−7.42 (m, 4H); EI MS *m/z* 693 (M + 1). Anal. ($C_{49}H_{68}N_4O_{10}$) C, H, N.

16: pale yellow oil; 58% yield; eluting solvent $CHCl_3$/EtOAc/petroleum ether/CH_3OH/aqueous 30% ammonia (4:3:2.5:0.5:0.05); ^1H NMR (DMSO-d_6) δ 1.18−1.81 (m, 22H), 2.22 (q, 2H), 2.65 (s, 2H), 2.86−3.18 (m, 8H), 3.85 (s, 4H), 4.15−4.35 (m, 10H), 6.48 (d, 4H), 6.88−7.21 (m, 8H), 7.41−7.58 (m, 4H); EI MS *m/z* 707 (M + 1). Anal. ($C_{50}H_{70}N_4O_{10}$) C, H, N.

General Procedures for the Synthesis of Methiodides 11−**13**. A solution of the appropriate compound (**6**, **7**, or **10**) as free base in acetone (15 mL) was treated with methyl iodide (1:10 molar ratio). After standing overnight at room temperature, the solvent was removed and the residue was triturated with ether to give a foam pale sticky solid in quantitative yield.

11: ^{1}H NMR (DMSO-d_6) δ 1.05−1.78 (m, 32H), 2.24 (t, 4H), 2.42 (t, 2H), 2.79 (s, 6H), 2.92 (t, 2H), 3.05−3.35 (m, 8H), 3.73−3.82 (m, 8H), 4.29 (d, 2H), 4.41 (s, 4H), 7.03 (t, 2H), 7.14 (d, 2H), 7.39−7.54 (m, 4H). Anal. ($C_{46}H_{76}I_2N_4O_4$) C, H, N.

12: ^{1}H NMR ($CDCl_3$) δ 0.98−1.95 (m, 34H), 2.35 (t, 4H), 2.49 (t, 2H), 2.95 (t, 2H), 3.08 (s, 6H), 3.35−3.75 (m, 8H), 3.73−3.91 (m, 8H), 4.49 (d, 2H), 4.71 (s, 4H), 6.98 (q, 4H), 7.38−7.52 (m, 2H), 7.68 (d, 2H). Anal. ($C_{47}H_{78}I_2N_4O_4$) C, H, N.

13: ^{1}H NMR (DMSO-d_6) δ 1.21−1.38 (m, 10H), 1.61−1.83 (m, 8H), 2.31 (t, 4H), 2.74 (s, 4H), 2.77 (s, 6H), 3.02−3.38 (m, 8H), 3.80 (s, 6H), 4.38 (s, 4H), 6.88−7.18 (m, 8H), 7.36−7.44 (m, 8H), 9.78 (s, 2H exchangeable with D_2O). Anal. ($C_{48}H_{68}I_2N_4O_4$) C, H, N.

Biology. Functional Antagonism at Guinea Pig Left Atria. Male guinea pigs (200−300 g) were killed by cervical dislocation. The heart was rapidly removed, and right and left atria were separated out and set up rapidly under 1 g of tension in 20 mL organ baths containing physiological salt solution (PSS) maintained at 30 °C and aerated with 5% CO_2−95% O_2.

The left atria were mounted in PSS of the following composition (mM): NaCl, 118; KCl, 4.7; $CaCl_2$, 2.52; $MgSO_4 \cdot 7H_2O$, 1.18; KH_2PO_4, 1.18; $NaHCO_3$, 23.8; glucose, 11.7. Tissues were stimulated through platinum electrodes by square-wave pulses (1 ms, 1 Hz, 5−10 V) (Tetra Stimulus, N. Zagnoni). Inotropic activity was recorded isometrically. Tissues were equilibrated for 2 h, and a cumulative concentration−response curve to APE was constructed. Concentration−response curves were constructed by cumulative addition of the reference agonist. The concentration of agonist in the organ bath was increased approximately 3-fold at each step, with each addition being made only after the response to the previous addition had attained a maximal level and remained steady. Following 30 min of washing, tissues were incubated with the antagonist for 1 h, and a new dose−response curve to the agonist was obtained. Contractions were recorded by means of a force displacement transducer connected to the MacLab system PowerLab/800. In addition parallel experiments in which tissues did not receive any antagonist were run in order to check any variation in sensitivity.

To quantify antagonist potency, pK_b values were calculated from the equation pK_b = log(DR − 1) − log [B], where DR is the ratio of EC_{50} values of agonist after and before treatment with 10 μM concentration of the antagonist [B].[24]

Inhibition of AChE and BChE. The method of Ellman et al. was followed.[22] Five different concentrations of each compound were used in order to obtain inhibition of AChE or BChE activity comprised between 20% and 80%. The assay solution consisted of a 0.1 M phosphate buffer pH 8.0, with the addition of 340 μM 5,5′-dithio-bis(2-nitrobenzoic acid), 0.035 unit/mL of human recombinant AChE or BChE derived from human serum (Sigma Chemical), and 550 μM of substrate (acetylthiocholine iodide or butyrylthiocholine iodide). Test compounds were added to the assay solution and preincubated at 37 °C with the enzyme for 20 min followed by the addition of substrate. Assays were done with a blank containing all components except AChE or BChE in order to account for nonenzymatic reaction. The reaction rates were compared, and the percent inhibition due to the presence of test compounds was calculated. Each concentration was analyzed in triplicate, and IC_{50} values were determined graphically from log concentration−inhibition curves.

Determination of Steady-State Inhibition Constant. To obtain estimates of the competitive inhibition constant K_i, reciprocal plots of 1/V versus 1/[S] were constructed at relatively low concentration of substrate (below 0.5 mM). The plots were assessed by a weighted least-squares analysis that assumed the variance of V to be a constant percentage of V for the entire data set. Slopes of these reciprocal plots were then plotted against **4** (range 0−1.93 nM) or donepezil concentration (range 0−65.1 nM) in a similar weighted analysis, and K_i was determined as the ratio of the replot intercept to the replot slope.

Reciprocal plots involving **4** or donepezil inhibition show both increasing slopes (decreased V_{max} at increasing inhibitor concentrations) and increasing intercepts (higher K_m) with higher inhibitor concentration. This pattern indicates mixed inhibition, arising from significant inhibitor interaction with both the free enzyme and the acetylated enzyme. Replots of the slope versus the concentration of **4** or donepezil gives estimate of competitive inhibition constant, $K_i = 5.67 \pm 0.15$ nM or $K_i = 20.5 \pm 3.3$ nM, respectively.

Thus, the pattern in the graphical representation shows **4** and donepezil able to bind to the peripheral anionic site as well as the active site of AChE.

Inhibition of AChE-Induced Aβ Aggregation. Aliquots of 2 μL of Aβ peptide, lyophilized from 2 mg mL^{-1} 1,1,1,3,3,3-hexafluoro-2-propanol solution and dissolved in DMSO, were incubated for 24 h at room temperature in 0.215 M sodium phosphate buffer (pH 8.0) at a final concentration of 230 μM. For coincubation experiments aliquots (16 μL) of AChE (final concentration 2.30 μM, Aβ/AChE molar ratio 100:1) and AChE in the presence of 2 μL of the tested inhibitor in 0.215 M sodium phosphate buffer pH 8.0 solution (final inhibitor concentration 100 μM) were added.

Blanks containing Aβ, AChE, and Aβ plus inhibitors in 0.215 M sodium phosphate buffer (pH 8.0) were prepared. The final volume of each vial was 20 μL. Each assay was run in duplicate. To quantify amyloid fibril formation, the thioflavin T fluorescence method was then applied.[28] The fluorescence intensities due to β-sheet conformation were monitored for 300 s at λ_{em} = 490 nm (λ_{ex} = 446 nm). The percent inhibition of the AChE-induced aggregation due to the presence of the test compound was calculated by the following expression: $100 - (IF_i/IF_o \times 100)$ where IF_i and IF_o are the fluorescence intensities obtained for Aβ plus AChE in the presence and in the absence of inhibitor, respectively, minus the fluorescence intensities due to the respective blanks.

Statistical Analysis. Data were analyzed using a pharmacological computer program.[30] Values are given as mean ± standard error of n independent observations. Student's t-test was used to assess the statistical significance of the difference between two means.

Acknowledgment. This research was supported by Grants from the University of Bologna (Funds for Selected Research Topics) and MIUR.

Supporting Information Available: Elemental analysis data of reported compounds. This material is available free of charge via the Internet at http://pubs.acs.org.

References

(1) Bachurin, S. O. Medicinal chemistry approaches for the treatment and prevention of Alzheimer's disease. *Med. Res. Rev.* **2003**, *23*, 48−88.
(2) Roberson, M. R.; Harrell, L. E. Cholinergic activity and amyloid precursor protein metabolism. *Brain Res. Rev.* **1997**, *25*, 50−69.
(3) Tariot, P. N.; Federoff, H. J. Current treatment for Alzheimer disease and future prospects. *Alzheimer Dis. Assoc. Disord.* **2003**, *17* (Suppl. 4), S105−113.
(4) Scarpini, E.; Scheltens, P.; Feldman, H. Treatment of Alzheimer's disease: current status and new perspectives. *Lancet Neurol.* **2003**, *2*, 539−547.
(5) Kasa, P.; Rakonczay, Z.; Gulya, K. The cholinergic system in Alzheimer's disease. *Prog. Neurobiol.* **1997**, *52*, 511−535.
(6) Gualtieri, F.; Dei, S.; Manetti, D.; Romanelli, M. N.; Scapecchi, S.; Teodori, E. The medicinal chemistry of Alzheimer's and Alzheimer-like diseases with emphasis on the cholinergic hypothesis. *Farmaco* **1995**, *50*, 489−503.
(7) Brufani, M.; Filocamo, L.; Lappa, S.; Maggi, A. New acetylcholinesterase inhibitors. *Drugs Future* **1997**, *22*, 397−410.
(8) Small, D. H.; Michaelson, S.; Sberna, G. Non-classical actions of cholinesterases: role in cellular differentiation, tumorigenesis and Alzheimer's disease. *Neurochem. Int.* **1996**, *28*, 453−483.
(9) Soreq, H.; Seidman, S. Acetylcholinesterase: new roles for an old actor. *Nat. Rev. Neurosci.* **2001**, *2*, 294−302.
(10) von Bernhardi, R.; Ramirez, G.; De Ferrari, G. V.; Inestrosa, N. C. Acetylcholinesterase induces the expression of the β-amyloid precursor protein in glia and activates glial cells in culture. *Neurobiol. Dis.* **2003**, *14*, 447−457.

(11) Rees, T.; Hammond, P. I.; Soreq, H.; Younkin, S.; Brimijoin, S. Acetylcholinesterase promotes beta-amyloid plaques in cerebral cortex. *Neurobiol. Aging* **2003**, *24*, 777−787.
(12) Alvarez, A.; Alarcon, R.; Opazo, C.; Campos, E. O.; Munoz, F. J.; Calderon, F. H.; Dajas, F.; Gentry, M. K.; Doctor, B. P.; De Mello, F. G.; Inestrosa, N. C. Stable complexes involving acetylcholinesterase and amyloid-β peptide change the biochemical properties of the enzyme and increase the neurotoxicity of Alzheimer's fibrils. *J. Neurosci. Res.* **1998**, *18*, 3213−3223.
(13) De Ferrari, G. V.; Canales, M. A.; Shin, I.; Weiner, L. M.; Silman, I.; Inestrosa, N. C. A structural motif of acetylcholinesterase that promotes amyloid β-peptide fibril formation. *Biochemistry* **2001**, *40*, 10447−10457.
(14) Chatonnet, A.; Lockridge, O. Comparison of butyrylcholinesterase and acetylcholinesterase. *Biochem. J.* **1989**, *260*, 625−634.
(15) Moran, M. A.; Mufson, E. J.; Gomez-Ramos, P. Colocalization of cholinesterases with beta amyloid protein in aged and Alzheimer's brains. *Acta Neuropathol.* **1993**, *85*, 362−369.
(16) Inestrosa, N. C.; Alvarez, A.; Perez, C. A.; Moreno, R. D.; Vicente, M.; Linker, C.; Casanueva, O. I.; Soto, C.; Garrido, J. Acetylcholinesterase accelerates assembly of amyloid-beta-peptides into Alzheimer's fibrils: possible role of the peripheral site of the enzyme. *Neuron* **1996**, *16*, 881−891.
(17) Massoulie, J.; Sussman, J.; Bon, S.; Silman, I. Structure and functions of acetylcholinesterase and butyrylcholinesterase. *Prog. Brain Res.* **1993**, *98*, 139−146.
(18) Melchiorre, C.; Antonello, A.; Banzi, R.; Bolognesi, M. L.; Minarini, A.; Rosini, M.; Tumiatti, V. Polymethylene tetraamine backbone as template for the development of biologically active polyamines. *Med. Res. Rev.* **2003**, *23*, 200−233.
(19) Bolognesi, M. L.; Minarini, A.; Budriesi, R.; Cacciaguerra, S.; Chiarini, A.; Spampinato, S.; Tumiatti, V.; Melchiorre, C. Universal template approach to drug design: polyamines as selective muscarinic receptor antagonists. *J. Med. Chem.* **1998**, *41*, 4150−4160.
(20) Melchiorre, C.; Andrisano, V.; Bolognesi, M. L.; Budriesi, R.; Cavalli, A.; Cavrini, V.; Rosini, M.; Tumiatti, V.; Recanatini, M. Acetylcholinesterase noncovalent inhibitors based on a polyamine backbone for potential use against Alzheimer's disease. *J. Med. Chem.* **1998**, *41*, 4186−4189.
(21) Tumiatti, V.; Rosini, M.; Bartolini, M.; Cavalli, A.; Marucci, G.; Andrisano, V.; Angeli, P.; Banzi, R.; Minarini, A.; Recanatini, M.; Melchiorre, C. Structure−activity relationships of acetylcholinesterase noncovalent inhibitors based on a polyamine backbone. 2. Role of the substituents on the phenyl ring and nitrogen atoms of caproctamine. *J. Med. Chem.* **2003**, *46*, 954−966.
(22) Ellman, G. L.; Courtney, K. D.; Andres, V.; Featherstone, R. M. A new rapid colorimetric determination of acetylcholinesterase activity. *Biochem. Pharmacol.* **1961**, *7*, 88−95.
(23) Minarini, A.; Bolognesi, M. L.; Budriesi, R.; Canossa, M.; Chiarini, A.; Spampinato, S.; Melchiorre, C. Design, synthesis, and biological activity of methoctramine-related tetraamines bearing an 11-acetyl-5,11-dihydro-6*H*-pyrido[2,3-*b*][1,4]benzodiazepin-6-one moiety: structural requirements for optimum occupancy of muscarinic receptor subtypes as revealed by symmetrical and unsymmetrical polyamines. *J. Med. Chem.* **1994**, *37*, 3363−3372.
(24) Van Rossum, J. M. Cumulative dose−response curves. II. Technique for the making of dose−response curves in isolated organs and the evaluation of drug parameters. *Arch. Int. Pharmacodyn. Ther.* **1963**, *143*, 299−330.
(25) Snape, M. F.; Misra, A.; Murray, T. K.; De Souza, R. J.; Williams, J. L.; Cross, A. J.; Green, A. R. A comparative study in rats of the in vitro and in vivo pharmacology of the acetylcholinesterase inhibitors tacrine, donepezil and NXX-066. *Neuropharmacology* **1999**, *38*, 181−193.
(26) Piazzi, L.; Rampa, A.; Bisi, A.; Gobbi, S.; Belluti, F.; Cavalli, A.; Bartolini, M.; Andrisano, V.; Valenti, P.; Recanatini, M. 3-(4-[[Benzyl(methyl)amino]methyl]phenyl)-6,7-dimethoxy-2*H*-2-chromenone (AP2238) inhibits both acetylcholinesterase and acetylcholinesterase-induced β-amyloid aggregation: a dual function lead for Alzheimer's disease therapy. *J. Med. Chem.* **2003**, *46*, 2279−2282.
(27) Inestrosa, N. C.; Alvarez, A.; Calderon, F. Acetylcholinesterase is a senile plaque component that promotes assembly of amyloid β-peptide into Alzheimer's filaments. *Mol. Psychiatry* **1996**, *1*, 359−361.
(28) Bartolini, M.; Bertucci, C.; Cavrini, V.; Andrisano, V. β-Amyloid aggregation induced by human acetylcholinesterase: inhibition studies. *Biochem. Pharmacol.* **2003**, *65*, 407−416.
(29) Giacobini, E. Selective inhibitors of butyrylcholinesterase: a valid alternative for therapy of Alzheimer's disease? *Drugs Aging* **2001**, *18*, 891−898.
(30) Motulsky, H. J. *Analyzing Data with GraphPad Prism*; GraphPad Software Inc.: San Diego, CA, 1999.

JM0494366